A Single-Shot Technique for Measuring

Broadband Two-Photon Absorption Spectra

in Solution

Prasenjit Srivastava and Christopher G. Elles*

Department of Chemistry, University of Kansas, Lawrence, Kansas 66045

E-mail: elles@ku.edu

Abstract

Applications involving two-photon activation, including two-photon fluorescence imaging, photo-

dynamic therapy, and 3D data storage, require precise knowledge of the two-photon absorption

(2PA) spectra of target chromophores. Broadband pump-probe spectroscopy using femtosecond

laser pulses provides wavelength-dependent 2PA spectra with absolute cross sections, but the mea-

surements are sometimes complicated by cross-phase modulation effects and dispersion of the

broadband probe. Here, we introduce a single-shot approach that eliminates artifacts from cross-

phase modulation and enables more rapid measurements by avoiding the need to scan the time

delay between the pump and probe pulses. The approach uses counter-propagating beams to auto-

matically integrate over the full interaction between the two pulses as they cross. We demonstrate

this single-shot approach for a common 2PA reference, coumarin 153 (C153), in three different

solvents using the output from a Yb:KGW laser. This approach provides accurate 2PA cross sec-

tions that are more reliable and easier to obtain compared with scanning pump-probe methods

using co-propagating laser beams. The single-shot method for broadband two-photon absorption

1

(BB-2PA) spectroscopy also has significant advantages compared with single-wavelength measurements, such as z-scan and two-photon fluorescence.

Introduction

Two-photon absorption (2PA) enables spatially localized excitation of target chromophores in applications ranging from two-photon imaging to photodynamic therapy. ^{1–4} Two-photon activation also allows longer-wavelength excitation compared with one-photon absorption, providing deeper tissue penetration and reduced damage to the surrounding material. ⁵ The development and implementation of novel chromophores for these applications requires simple methods for measuring 2PA spectra with accurate cross sections across a wide range of wavelengths. Typical methods for obtaining 2PA cross sections include z-scan ^{6,7} and two-photon excited fluorescence (2PEF). ^{8,9} However, both of these methods involve single-beam measurements that require tuning the monochromatic light source to obtain the full 2PA spectrum of a molecule. Variation of the spatial or temporal profile of the pump beam with wavelength can result in systematic variation of the measured spectrum that can be difficult to diagnose. Additionally, the z-scan technique is susceptible to contributions from other non-linear phenomena, whereas 2PEF is an indirect method for measuring 2PA cross sections that depends on prior knowledge of the fluorescence quantum yield and typically requires an external standard for calibration of the detection efficiency. ¹⁰

In contrast with single-beam measurements, broadband 2PA (BB-2PA) spectroscopy using a pump-probe approach provides continuous spectra across a wide range of wavelengths. ^{11–15} The BB-2PA spectrum is obtained from the wavelength-dependent attenuation of the probe due to simultaneous absorption of individually non-resonant pump and probe photons when the pulses are overlapped in the sample. We recently showed that stimulated Raman scattering (SRS) from the solvent provides a robust internal standard to calibrate the measurement of 2PA cross sections using the broadband approach. ¹⁶ The SRS signal depends on the same experimental parameters as 2PA, including the intensity-dependent temporal and spatial overlap of pump and probe pulses,

and therefore serves as a reliable reference point for determining absolute 2PA cross sections.

In this contribution, we introduce an important extension of the BB-2PA technique that enables single-shot measurements for faster data acquisition and decreased sensitivity to dispersive artifacts. Specifically, we use counter-propagating pump and probe beams to automatically integrate over the full temporal profile of the two pulses as they cross in the sample. Using this single-shot approach, the full 2PA spectrum can be measured without scanning a translation stage to account for dispersion of the probe light, which is one of the biggest limitations of broadband 2PA using a traditional pump-probe configuration. The single-shot method also eliminates the need for manual integration of the time-dependent signal in order to remove cross-phase modulation (XPM) effects. ^{16–18} In order to demonstrate the benefits of this approach we report the 2PA spectrum of coumarin 153 (C153) in solution. We use the results from more than 80 independent measurements to demonstrate the accuracy and reproducibility of the 2PA spectra measured using this single-shot approach.

Methods

We measure single-shot BB-2PA spectra using an amplified Yb:KGW laser (Light Conversion, Carbide) operating at 1 kHz. The laser fundamental at 1030 nm was used as the pump beam, with a synchronized chopper wheel blocking alternating pump pulses for shot-to-shot background subtraction. A small portion of the laser output was used to obtain broadband probe pulses via super-continuum generation in a YAG crystal. ^{19,20} The two beams propagate in opposite directions through a 5 mm cuvette containing the sample solution, where they cross at a small angle ($< 5^{\circ}$). After the sample, the probe beam passes into a 1/8 m imaging spectrograph (Newport, MS127i) with a 300 line/mm grating that disperses the light onto a 256 pixel photodiode array (Hamamatsu, S3901-256Q). We obtain the 2PA spectrum from the differential absorption, $\Delta A(\lambda_{pr}) = -\log(T_{ON}/T_{OFF})$, where T_{ON} and T_{OFF} are the intensity of the transmitted probe beam at wavelength λ_{pr} when measured with and without the pump pulse simultaneously incident on the sample.

The overlap length of the counter-propagating pulses ($\sim 300 \ \mu m$) is determined by the duration of the (chirped) probe pulse, and we set the relative time delay such that each pump and probe pair overlap entirely within the sample (see Figure S1 of the SI). We typically average 250k shots per spectrum without changing the time delay. The sample solutions consist of 15-20 mM coumarin 153 (MilliporeSigma, >99%) in methanol, DMSO, or toluene.

The 2PA cross section, $\sigma_{2PA}(\lambda)$, is proportional to the differential absorption signal, ^{13,21}

$$\sigma_{2PA}(\lambda) = \frac{1000 \cdot \ln 10 \cdot hc}{\lambda_{pu} \cdot E_{pu} \cdot f \cdot conc. \cdot N_A} \cdot \Delta A_{2PA}(\lambda_{pr}) \tag{1}$$

where E_{pu} is the energy of the pump pulses (in J), f is the intensity-weighted overlap of the pump and probe beams (in cm⁻¹·s⁻¹), conc. is the molar sample concentration, and N_A is Avogadro's number. The units of $\sigma_{2PA}(\lambda)$ are Göppert-Mayer (1 GM = 10^{-50} cm⁴·s·molec.⁻¹·photon⁻¹) and we report the cross section as a function of the transition wavelength, λ , which is equivalent to the wavelength of light that would achieve the same total excitation energy using a single photon rather than the sum of pump and probe photons at wavelengths λ_{pu} and λ_{pr} , respectively. We use the SRS signal of the solvent as an internal standard to obtain the overlap factor, f, as described previously. ¹⁶

In our earlier work using co-propagating pump and probe pulses we obtained a spatial overlap factor, f_V , in units of cm⁻¹ after manually integrating the differential absorption signal over the pump-probe delay time. ¹⁶ However, the temporal overlap (*i.e.*, convolution) of the pump and probe pulses is automatically encoded into the overlap factor when using counter-propagating pulses, resulting in units of cm⁻¹·s⁻¹, and does not need to be considered as long as the pulse widths are short compared with the path length over which they interact. For both cases, counter- and co-propagating pulses, the overlap parameter is identical for 2PA and SRS, therefore we scale the 2PA spectrum using known Raman scattering cross sections of the solvent in order to obtain absolute 2PA cross sections for the solute. The accuracy of the 2PA cross sections determined using this method only depends on the accuracy of the solvent SRS cross section and the solute concentration, because all other experimental parameters (including pump pulse energy and spatial overlap) are

essentially eliminated from the determination of σ_{2PA} . ¹⁶ The SRS cross section is a fundamental property of the solvent, and therefore can be known very precisely. Furthermore, this approach allows solute 2PA cross sections to be easily updated if more accurate Raman cross sections are determined at a later time. In this contribution, we use differential Raman cross sections of 0.86, 2.45, and 3.27×10^{-30} cm²·molec. ⁻¹sr⁻¹ for the CH stretching bands of methanol, DMSO, and toluene, respectively, based on new measurements with an estimated uncertainty of 15%.

Results and Discussion

Figure 1 shows the BB-2PA spectrum that we obtain for C153 in methanol using counter-propagating pump and probe pulses. The broadband probe covers a wavelength range of 550-850 nm. By passing through the sample in opposite directions, the pump pulse interacts with the full range of wavelengths in the probe pulse on every laser shot, automatically providing the time-integrated absorption signal. Importantly, this time-integrated signal is independent of group-velocity dispersion and also eliminates XPM effects caused by the time-dependent interaction of the pump and probe pulses. ^{16–18} The raw signal in Figure 1A (red line) includes contributions from both 2PA of the solute and SRS of the solvent. We remove the Raman contribution by subtracting the SRS signal of the neat solvent measured under identical conditions (blue line) in order to obtain the pure 2PA spectrum of C153 (yellow line). Figure 1B shows the solvent-subtracted 2PA spectrum on an absolute scale in units of GM that we determine from the magnitude of the SRS contribution. The combined energy of the 1030 nm pump and broadband probe pulses covers a 2PA transition wavelength range of 353-475 nm.

For comparison with the single-shot approach, Figure S6 of the SI shows how we obtain the 2PA spectrum using co-propagating pump and probe pulses. In the case of co-propagating beams, the pump and probe pulses do not automatically integrate over the full interaction time, therefore we manually scan the pump-probe delay over a range of 2.5 ps (in 10 fs steps, typically 12k shots per time delay) and then integrate the signal at each probe wavelength in order to account for

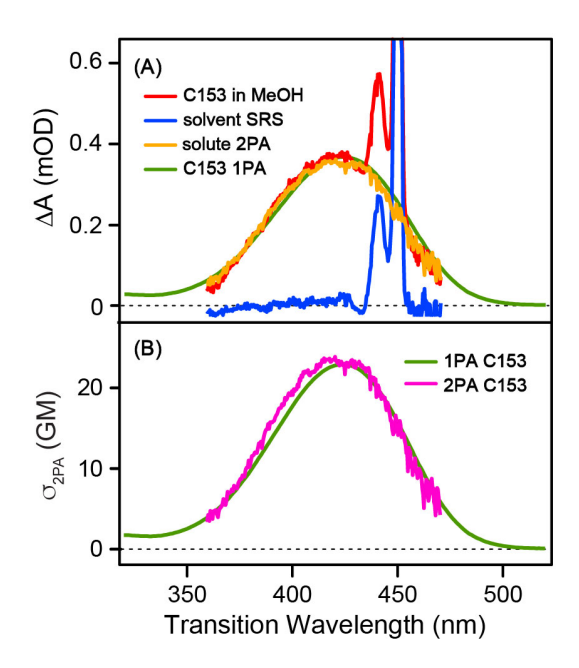


Figure 1: Single-shot BB-2PA spectrum of C153 in MeOH. (A) Differential absorption spectrum for a 25 mM sample of C153 (red) compared with the neat solvent (blue), and the solvent-subtracted signal that represents only 2PA from C153 (yellow). (B) Calibrated 2PA spectrum on an absolute scale. The green lines are the 1PA spectrum of C153 for comparison.

group-velocity dispersion of the white-light probe pulses. ¹⁶ Manual integration of the pump-probe delay over the full range of the interaction is an extra step compared with the single-shot approach using counter-propagating beams. The manual integration also introduces additional noise from shot-to-shot fluctuations and sometimes results in incomplete cancelation of the XPM signal. In the case of counter-propagating beams, each pair of laser pulses samples the full pump-probe interaction, which eliminates the need for manual integration and reduces the time spent averaging the signal at delays for which the pump and probe are not fully overlapped in time at any given probe wavelength. Thus, the counter-propagating (single-shot) approach reduces the total data acquisition time by more than 90% compared with the co-propagating approach, 250k vs 3M total laser shots, while achieving a similar signal-to-noise level.

In order to demonstrate the reproducibility of the single-shot BB-2PA approach, we measured 84 independent scans of C153 in methanol (see Figure 2A). The independent scans were obtained

on different days or after realignment of the laser, often following significant reconfiguration of the pump-probe arrangement. The average cross section at the absorption maximum is 26.5 ± 0.4 GM, where the uncertainty is the standard deviation of the mean. Figure 2B shows 17 independent measurements using the co-propagating pump-probe technique, for which the average cross section is 28.9 ± 2.6 GM. Although the cross sections obtained using the two approaches agree within error, the single-shot measurement has smaller variation between scans compared with the co-propagating measurements (standard deviation of 3.5 versus 10.8 GM). The larger variation in the latter case is largely due to residual baselines caused by XPM effects and other errors associated with manual integration. 22,23 In favorable cases, contributions from XPM are completely removed by integrating the transient signal over the time-delay between the pump and probe pulses, $^{16-18}$ but the XPM signal can be up to an order of magnitude larger than the 2PA signal, therefore small shotto-shot fluctuations result in incomplete cancellation of this time-dependent signal during manual integration. In contrast, counter-propagating pump and probe pulses self integrate as they cross each other in the sample, thereby effectively removing XPM on a shot-by-shot basis.

The dark red and purple lines in Figure 2 show the 2PA spectra that we obtain by averaging 83 of the independent counter-propagating scans (we exclude one obvious outlier) and all 17 of the co-propagating scans, respectively. Averaging all 83 scans from the measurements with counter-propagating beams reveals that the 2PA spectrum has a small, but distinct blue shift compared with the 1PA spectrum of C153 in methanol. This shift may originate from slightly different Franck-Condon factors for one- and two-photon excitation. However, some of the apparent shift may also reflect an increase of the non-degenerate 2PA cross section at shorter wavelengths due to pre-resonance enhancement effects becoming more significant as the probe wavelength approaches the lowest-energy absorption band. Elayan and Brown ecently described pre-resonance enhancement effects in non-degenerate 2PA spectra and showed that the cross section can increase by as much as a factor of 2 across the spectrum, which could result in an apparent shift of the absorption band in the non-degenerate 2PA spectrum. Although we are uncertain of the exact reason for the slightly blue-shifted 2PA band in C153, a slight narrowing relative to the 1PA spectrum suggests

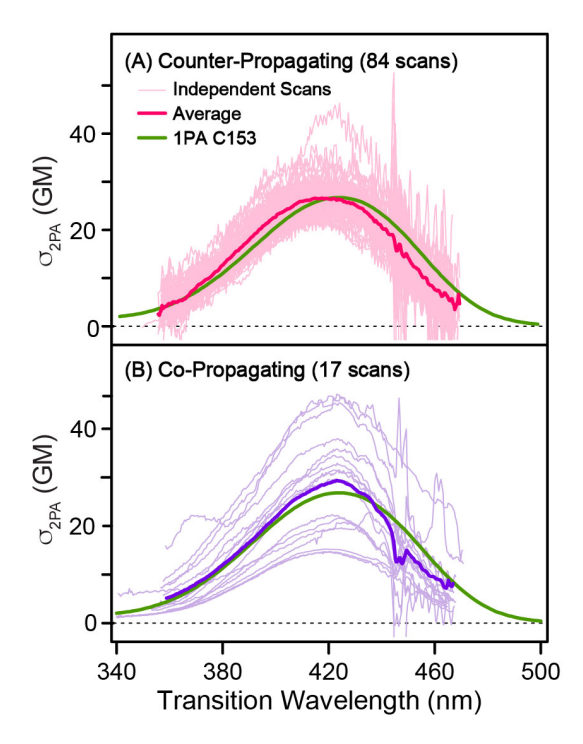


Figure 2: BB-2PA spectroscopy of C153 in methanol using (A) counter- and (B) co-propagating laser pulses. Lighter colored lines are independent scans, dark lines are the averages (see text), and green lines are the 1PA spectrum for comparison.

that Frank-Condon effects may be at least partially responsible, as differences in the vibronic overlap are expected to play a more significant role on the lower-energy side of the absorption band.²⁴ We rule out solvent heating effects, because the blue shift that we observe is inconsistent with hot-band absorption, which typically shifts the spectrum to longer wavelengths, and also because we do not observe any intensity dependence of the 2PA spectrum (see Figure S2 in the SI).

We also measured the 2PA spectrum of C153 in DMSO and toluene (Figure 3), for which de Reguardati et al.⁸ reported 2PA cross sections across a wide range of wavelengths using the degenerate 2PEF method. The resulting 2PA spectra from those authors closely match the shapes of the spectra from our non-degenerate BB-2PA measurements, including a significant narrowing and shifting of the absorption band in toluene compared with the polar solvents. This solvatochromic shift of the 2PA band highlights the importance of measuring the full 2PA spectrum, rather than a single point, as is often the case in z-scan and 2PEF measurements. The figure also shows the 1PA spectra for comparison (green lines), but we note that the 2PA spectrum does not always follow

the 1PA spectrum, therefore solvatochromic shifts cannot always be anticipated based on a simple comparison of the two.

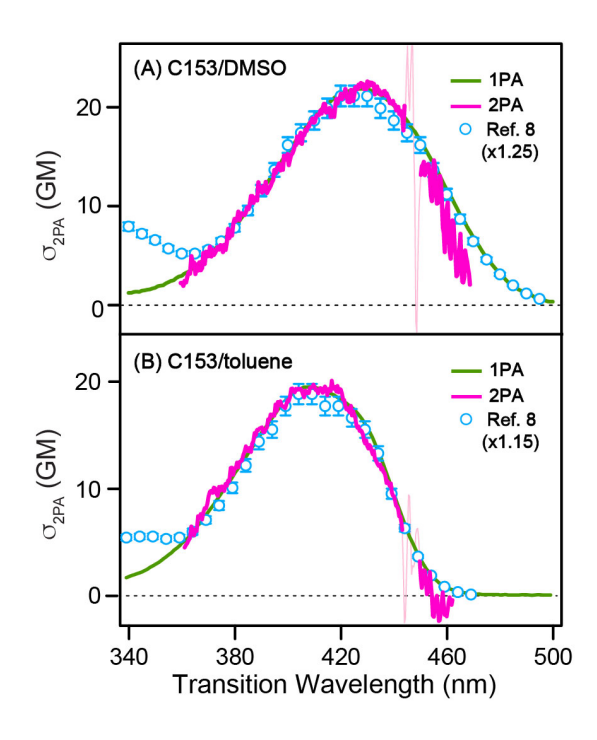


Figure 3: 2PA spectrum of C153 in (A) DMSO and (B) toluene. Pink lines are single-shot BB-2PA spectra, blue markers are from 2PEF measurements in Ref. 8, and green lines are the 1PA spectra for comparison.

While the spectral shapes of our BB-2PA measurements are in good agreement with the 2PEF measurements, there is a discrepancy in the absolute cross sections considering that the single-beam measurements should give cross sections that are one-half the value measured using two-beam methods. ^{27,28} The BB-2PA spectra in Figure 3 represent single scans, rather than an average over many independent measurements. Therefore the uncertainty in the absolute 2PA cross sections for these spectra is determined by the standard deviation (rather than the standard deviation of the mean) from our statistical analysis of the results in Figure 2, which is about 15% of the total signal. While this uncertainty could explain some of the difference between our absolute 2PA cross sections and those reported by de Reguardati, et al., ⁸ some of the remaining difference may be a result of systematic error in the SRS cross sections. The Raman cross sections that we use here come from new, frequency-dependent measurements that we estimate to be accurate within 15%

at 1030 nm, giving an overall uncertainty of \sim 21% in our absolute σ_{2PA} values.

We note that our earlier BB-2PA measurements using co-propagating beams and an excitation wavelength of 1158 nm used SRS cross sections that were extrapolated from 488 nm and did not account for pre-resonance enhancement effects in the solvent Raman spectrum. ¹⁶ In other words, our earlier measurements overestimated the 2PA cross sections by about a factor of 2.2. This highlights the benefits of obtaining 2PA cross sections using the solvent Raman bands as an internal standard, because the absolute value of the 2PA spectrum can be updated as new Raman cross sections become available. In any case, the uncertainty across the spectrum of any single scan using the BB-2PA approach is much lower than the uncertainty in the value of the absolute cross section. Considering that each BB-2PA spectrum takes only ~4 min to record using the single-shot approach, compared with up to an hour per scan for co-propagating pulses and up to 4 hours per point for the 2PEF method, ⁸ the counter-propagating approach represents a considerable improvement in 2PA measurement capabilities.

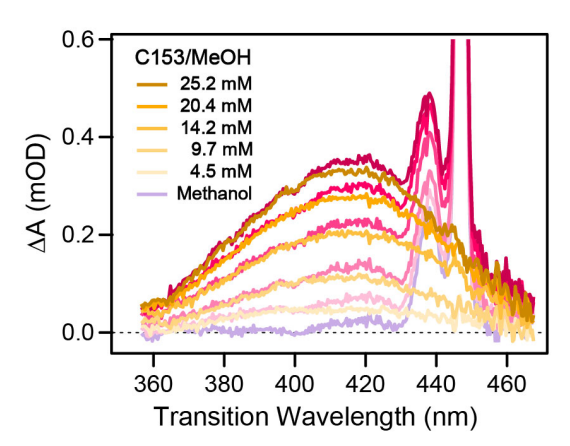


Figure 4: Single-shot 2PA spectra for various concentrations of C153 in methanol. Red lines are the differential absorption of each sample, yellows lines are the solvent-subtracted spectra.

In order to demonstrate the sensitivity of the single-shot approach, we measured the 2PA spectrum of C153 in methanol as a function of concentration. Figure 4 shows the raw differential absorption spectra and the solvent-subtracted signals at concentrations ranging from 4.5 to 25.2 mM. As expected, the 2PA signal increases linearly with the concentration of C153 (see Figure S3 in the SI), whereas the methanol SRS signal remains constant. Even with the signal-to-noise that

we obtain from a single scan (\sim 4 min of averaging), we are able to distinguish the spectrum of C153 down to a few mM concentration. With additional averaging, the detection limit could be lowered even further. For one hour of averaging, we estimate a limit of <0.5 GM at a concentration of 25 mM, or a concentration limit of \sim 25 μ M for a chromophore with σ_{2PA} = 500 GM. This result shows that the single-shot approach is sensitive enough to obtain BB-2PA spectra within a reasonable amount of time even for relatively weak two-photon chromophores.

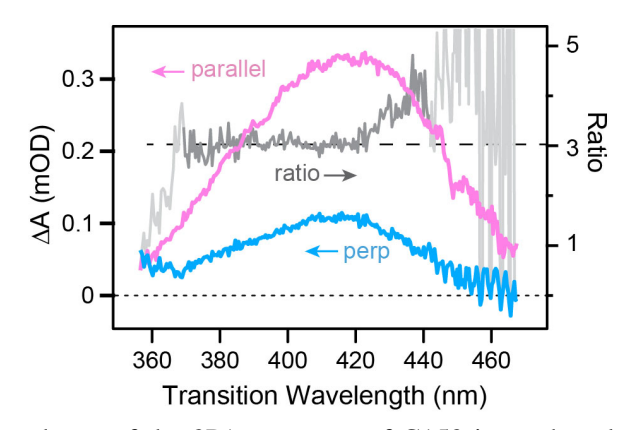


Figure 5: Polarization dependence of the 2PA spectrum of C153 in methanol. The ratio for parallel and perpendicular polarization reflects the symmetry of the underlying transition.

Finally, one of the key benefits of BB-2PA spectroscopy is the ability to independently control the properties of the two photons being absorbed, including their relative polarization. Measuring 2PA spectra with different polarization components provides valuable information about the symmetry of the excited state and can help distinguish competing contributions from overlapping transitions. ^{29–31} To illustrate this capability using the single-shot approach, Figure 5 compares the 2PA spectrum for C153 in methanol using parallel and perpendicular relative polarization of the pump and probe light. The ratio of the 2PA signals has a constant value of 3.0 across most of the 2PA band, deviating only where the solvent SRS bands overlap the 2PA spectrum (> 430 nm). The constant polarization ratio suggests that a single transition to a totally symmetric excited state is responsible for the absorption band, ³² consistent with TD-DFT calculations showing that C153 has only one excited state in this energy range (Figure S7 in the SI). The ease with which we obtain the polarization ratio across the entire 2PA spectrum further highlights the value of the single-shot

BB-2PA approach.

Conclusion

The broadband pump-probe method using counter-propagating pulses provides accurate 2PA cross sections in a fraction of the time of the scanning pump-probe method using co-propagating pulses. This single-shot approach is more efficient, requires less data processing, and significantly reduces the impact of nonlinear artifacts. The BB-2PA approach also has significant advantages over single-wavelength measurements, including z-scan and 2PEF, because it avoids the need to scan the excitation wavelength across the full 2PA spectrum and enables more accurate measurements using solvent SRS bands as an internal standard. The 2PA cross sections obtained using the single-shot technique are in good agreement with literature and reveal subtle spectroscopic features including a weak blue-shift of the C153 2PA spectrum compared with the 1PA spectrum. Such features can be difficult to observe with techniques like z-scan and 2PEF where the 2PA spectrum is obtained by tuning a single wavelength laser. This simplified single-shot approach should make accurate 2PA measurements more accessible and therefore will be beneficial in the development of new chromophores for applications such as two-photon imaging or catalysis. 33,34

Acknowledgement

This material is based upon work supported by the National Science Foundation under grant number CHE-1905334. The authors thank Chase Courbot for measuring the time-dependence of the 2PA signal using counter-propagating beams.

Supporting Information Available

Examples of the time, power, and concentration dependence of the 2PA signal; using solvent SRS as an internal standard; subtracting solvent contributions for DMSO and toluene; comparison with

the BB-2PA approach using co-propagating laser beam; and calculated 1PA transitions of C153.

References

- (1) Zhai, B.; Hu, W.; Zhai, S.; Liang, T.; Liu, Z. Two-photon imaging for visualizing polarity in lipid droplets during chemotherapy induced ferroptosis. *Talanta* **2023**, *256*, 124304.
- (2) Kim, H. M.; Cho, B. R. Small-molecule two-photon probes for bioimaging applications. *Chem. Rev.* **2015**, *115*, 5014–5055.
- (3) Wei, X.; Cui, W. B.; Qin, G. Y.; Zhang, X. E.; Sun, F. Y.; Li, H.; Guo, J. F.; Ren, A. M. Theoretical investigation of Ru(II) complexes with long lifetime and a large two-photon absorption cross-section in photodynamic therapy. *J. Med. Chem.* **2023**, *66*, 4167–4178.
- (4) Wang, S.; Wu, W.; Manghnani, P.; Xu, S.; Wang, Y.; Goh, C. C.; Ng, L. G.; Liu, B. Polymerization-Enhanced Two-Photon Photosensitization for Precise Photodynamic Therapy. *ACS Nano* **2019**, *13*, 3095–3105.
- (5) Bolze, F.; Jenni, S.; Sour, A.; Heitz, V. Molecular photosensitisers for two-photon photodynamic therapy. *Chem. Comm.* **2017**, *53*, 12857–12877.
- (6) Ajami, A.; Husinsky, W.; Liska, R.; Pucher, N. Two-photon absorption cross section measurements of various two-photon initiators for ultrashort laser radiation applying the Z-scan technique. J. Opt. Soc. Am. B, 2010, 27, 2290–2299.
- (7) Ajami, A.; Husinsky, W.; Tromayer, M.; Gruber, P.; Liska, R.; Ovsianikov, A. Measurement of degenerate two-photon absorption spectra of a series of developed two-photon initiators using a dispersive white light continuum Z-scan. *Appl. Phys. Lett.* **2017**, *111*, 07901.
- (8) de Reguardati, S.; Pahapill, J.; Mikhailov, A.; Stepanenko, Y.; Rebane, A. High-accuracy reference standards for two-photon absorption in the 680–1050 nm wavelength range. *Opt. Express*, **2016**, *24*, 9053.

- (9) Xu, C.; Webb, W. W. Measurement of two-photon excitation cross sections of molecular fluorophores with data from 690 to 1050 nm. *J. Opt. Soc. Am. B*, **1996**, *13*, 481–491.
- (10) Sun, C. L.; Liao, Q.; Li, T.; Li, J.; Jiang, J. Q.; Xu, Z. Z.; Wang, X. D.; Shen, R.; Bai, D. C.; Wang, Q.; Zhang, S. X.; Fu, H. B.; Zhang, H. L. Rational design of small indolic squaraine dyes with large two-photon absorption cross section. *Chem. Sci.* 2015, 6, 761–769.
- (11) Negres, R. A.; Hales, J. M.; Kobyakov, A.; Hagan, D. J.; Van Stryland, E. W. Experiment and analysis of two-photon absorption spectroscopy using a white-light continuum probe. *IEEE J. Quantum Electron.*, **2002**, *38*, 1205–1216.
- (12) Negres, R. A.; Hales, J. M.; Kobyakov, A.; Hagan, D. J.; Van Stryland, E. W. Two-photon spectroscopy and analysis with a white-light continuum probe. *Opt. Lett.*, **2002**, *27*, 270–272.
- (13) Yamaguchi, S.; Tahara, T. Two-photon absorption spectrum of all-trans retinal. *Chem. Phys. Lett.*, **2003**, *376*, 237–243.
- (14) Hosoi, H.; Tayama, R.; Takeuchi, S.; Tahara, T. Solvent dependence of two-photon absorption spectra of the enhanced green fluorescent protein (eGFP) chromophore. *Chem. Phys. Lett.*, **2015**, *630*, 32–36.
- (15) Houk, A. L.; Zheldakov, I. L.; Tommey, T. A.; Elles, C. G. Two-photon excitation of transstilbene: Spectroscopy and dynamics of electronically excited states above S₁. *J. Phys. Chem. B*, **2015**, *119*, 9335–9344.
- (16) Srivastava, P.; Stierwalt, D. A.; Elles, C. G. Broadband two-photon absorption spectroscopy with stimulated Raman scattering as an internal standard. *Anal. Chem.* **2023**, *95*, 13227–13234.
- (17) Ekvall, K.; van der Meulen, P.; Dhollande, C.; Berg, L.-E.; Pommeret, S.; Naskrecki, R.; Mialocq, J.-C. Cross phase modulation artifact in liquid phase transient absorption spectroscopy. *J. Appl. Phys.* **2000**, *87*, 2340–2352.

- (18) Bresci, A.; Guizzardi, M.; Valensise, C. M.; Marangi, F.; Scotognella, F.; Cerullo, G.; Polli, D. Removal of cross-phase modulation artifacts in ultrafast pump-probe dynamics by deep learning. *APL Photonics* **2021**, *6*, 076104.
- (19) Dubietis, R. A.; Tamošauskas, G.; Šuminas, R.; Jukna, V.; Couairon, A. Ultrafast supercontinuum generation in bulk condensed media. *Lith. J. Phys.* **2017**, *57*, 113–157.
- (20) Calendron, A.-L.; Çankaya, H.; Cirmi, G.; Kärtner, F. X. White-light generation with sub-ps pulses. *Opt. Express*, **2015**, *23*, 13866.
- (21) Elles, C. G.; Rivera, C. A.; Zhang, Y.; Pieniazek, P. A.; Bradforth, S. E. Electronic structure of liquid water from polarization-dependent two-photon absorption spectroscopy. *J. Chem. Phys.* **2009**, *130*, 084501.
- (22) Alfano, R. R.; Ho, P. P. Self-, cross-, and induced-phase modulations of ultrashort laser pulse propagation. *IEEE J. Quantum Electron.*, **1988**, *24*, 351–364.
- (23) Agrawal, P.; Baldeck, P. L.; Alfano, R. R. Temporal and spectral effects of cross-phase modulation on copropagating ultrashort pulses in optical fibers. *Phys. Rev. A*, **1989**, *40*, 5063–5072.
- (24) Drobizhev, M.; Tillo, S.; Makarov, N. S.; Hughes, T. E.; Rebane, A. Absolute two-photon absorption spectra and two-photon brightness of orange and red fluorescent proteins. *J. Phys. Chem. B*, **2009**, *113*, 855–859.
- (25) Drobizhev, M.; Makarov, N. S.; Tillo, S. E.; Hughes, T. E.; Rebane, A. Two-photon absorption properties of fluorescent proteins. *Nat. Methods*, **2011**, *8*, 393–399.
- (26) Elayan, I. A.; Brown, A. Degenerate and non-degenerate two-photon absorption of coumarin dyes. *Phys. Chem. Chem. Phys.* **2023**, *25*, 16772–16780.
- (27) Rumi, M.; Perry, J. W. Two-photon absorption: an overview of measurements and principles. *Adv. Opt. Photonics* **2010**, *2*, 451.

- (28) Beerepoot, M. T. P.; Friese, D. H.; List, N. H.; Kongsted, J.; Ruud, K. Benchmarking two-photon absorption cross sections: performance of CC2 and CAM-B3LYP. *Phys. Chem. Chem. Phys.* **2015**, *17*, 19306–19314.
- (29) Monson, P. R.; McClain, W. M. Polarization dependence of the two-photon absorption of tumbling molecules with application to liquid 1-chloronaphthalene and benzene. *J. Chem. Phys.*, **1970**, *53*, 29–37.
- (30) McClain, W. M. Excited state symmetry assignment through polarized two-photon absorption studies of fluids. *J. Chem. Phys.*, **1971**, *55*, 2789–2796.
- (31) De Wergifosse, M.; Houk, A. L.; Krylov, A. I.; Elles, C. G. Two-photon absorption spectroscopy of trans-stilbene, cis-stilbene, and phenanthrene: Theory and experiment. *J. Chem. Phys.*, **2017**, *146*, 144305.
- (32) De Wergifosse, M.; Elles, C. G.; Krylov, A. I. Two-photon absorption spectroscopy of stilbene and phenanthrene: Excited-state analysis and comparison with ethylene and toluene. *J. Chem. Phys.* **2017**, *146*, 174102.
- (33) Kundu, B. K.; Han, C.; Srivastava, P.; Nagar, S.; White, K. E.; Krause, J. A.; Elles, C. G.; Sun, Y. Trifluoromethylative bifunctionalization of alkenes via a bibenzothiazole-derived photocatalyst under both visible- and near-infrared-light irradiation. *ACS Catal.* **2023**, *13*, 8119–8127.
- (34) Chen, R.; Qiu, K.; Leong, D. C.; Kundu, B. K.; Zhang, C.; Srivastava, P.; White, K. E.; Li, G.; Han, G.; Guo, Z.; Elles, C. G.; Diao, J.; Sun, Y. A general design of pyridinium-based fluorescent probes for enhancing two-photon microscopy. *Biosens. Bioelectron.* **2023**, *239*, 115604.

TOC Graphic

